The Journal of Experimental Biology 206, 3125-3138

doi:10.1242/jeb.00514

Optimization of bone growth and remodeling in response to loading in tapered mammalian limbs

Daniel E. Lieberman[1,*], Osbjorn M. Pearson[2], John D. Polk[1], Brigitte Demes[3] and A. W. Crompton[4]

[1]*Peabody Museum, Harvard University, 11 Divinity Avenue, Cambridge Massachusetts 02138, USA,* [2]*Department of Anthropology, University of New Mexico, Albuquerque, New Mexico, 87131, USA,* [3]*Department of Anatomical Sciences, Health Sciences Center, State University of New York, Stony Brook, New York, 11794, USA* and [4]*Museum of Comparative Zoology, Harvard University, 26 Oxford St., Cambridge, Massachusetts, 02138, USA*

*Author for correspondence (e-mail: danlieb@fas.harvard.edu)

Accepted 27 May 2003

Summary

How bones respond dynamically to mechanical loading through changes in shape and structure is poorly understood, particularly with respect to variations between bones. Structurally, cortical bones adapt *in vivo* to their mechanical environments primarily by modulating two processes, modeling and Haversian remodeling. Modeling, defined here as the addition of new bone, may occur in response to mechanical stimuli by altering bone shape or size through growth. Haversian remodeling is thought to be an adaptation to repair microcracks or prevent microcrack propagation. Here, we examine whether cortical bone in sheep limbs modulates periosteal modeling and Haversian remodeling to optimize strength relative to mass in hind-limb midshafts in response to moderate levels of exercise at different growth stages. Histomorphometry was used to compare rates of periosteal growth and Haversian remodeling in exercised and sedentary treatment groups of juvenile, subadult and young adult sheep. *In vivo* strain data were also collected for the tibia and metatarsal midshafts of juvenile sheep. The results suggest that limb bones initially optimize responses to loading according to the varying power requirements associated with adding mass at different locations. In juveniles, exercise induces higher rates of periosteal modeling in proximal midshafts and higher rates of Haversian remodeling in distal midshafts. Consequently, distal element midshafts experience higher strains and, presumably, have lower safety factors. As animals age, periosteal modeling rates decline and Haversian remodeling rates increase, but moderate levels of mechanical loading stimulate neither process significantly.

Key words: bone, periosteal modeling, Haversian re-modeling, growth, sheep, strain.

Introduction

In most mammals, especially those adapted for cursoriality, distal limb bones are thinner than more proximal bones, giving the limb skeleton a tapered shape (Smith and Savage, 1956; Alexander, 1980, 1996; Hildebrand, 1985; Lieberman and Pearson, 2001; Currey, 2002). In sheep, for example, midshaft cortical areas decrease about 16% between the femur and tibia, and 24% between the tibia and metatarsal. Limb tapering is generally thought to save energy by reducing a limb's moment of inertia (Hildebrand, 1985). How much energy is saved by distal tapering has been the subject of debate, but is probably considerable in most species. While Taylor et al. (1974) found that three species (cheetah, gazelle and goats) with different limb configurations had similar energy costs (V_{O_2} g^{-1} h^{-1}) over a range of speeds, the conclusions of the study may be flawed because the animals were not run at comparable speeds. The results of Taylor et al. (1974) contradict not only theoretical predictions (for example, see Hildebrand, 1985), but also more controlled studies such as by Myers and Steudel (1985), who found that redistributing 3.6 kg from the thigh to the ankles in trained humans increases the metabolic cost of running at 2.68 m s^{-1} by 15%.

Limb tapering may save energy during swing, but may also affect bone strength during stance. Limbs during stance are usually modeled as cylinders subject to a combination of bending and axial compression from body mass and ground reaction forces. At midstance, when ground reaction forces (GRFs) are typically highest and approximately vertical, bending stress/strain at midshaft (the likely location of maximum bending) is a function of many factors, including the magnitude and orientation of GRF relative to the element and the cross-sectional and the material properties of the bone (Biewener et al., 1983). Distal tapering, therefore, leads not

only to higher compressive strains because of smaller cortical areas, but also to potentially higher bending strains because of decreased second moments of area (I) available to resist the bending moments that account for a high proportion of midshaft strains (Bertram and Biewener, 1988).

High strains in tapered distal bones can pose structural problems, especially because repeated high strains can lead to the generation and propagation of fatigue damage (e.g. microcracks), which contribute to mechanical failure (see Martin et al., 1998; Currey, 2002). Mammals have several potential adaptations to distal tapering, of which the two best documented are changes in gait and element length with increasing body mass. Larger mammals tend to orient their distal limb bones more in line with GRFs at peak loading, thereby increasing the proportion of axial compression relative to bending (Gambaryan, 1974; Biewener, 1983; Biewener et al., 1988; Polk, 2002). Larger mammals also tend to compensate for geometric scaling of midshaft diameters by shortening distal limb elements relative to total limb length l, thereby reducing bending moments (Smith and Savage, 1956; Gambaryan, 1974; Alexander, 1977; Jungers, 1985; Bertram and Biewener, 1992). Other potential adaptations to limb tapering are less well documented. While bone curvature across mammals decreases slightly but significantly with body mass M ($\propto M^{-0.09}$), helping to reduce bending stresses (Biewener, 1983), distal elements are not straighter than proximal elements (Bertram and Biewener, 1988). In addition, some studies (see MacKelvie et al., 2002) show a positive correlation between exercise and bone mineral density, which increases stiffness, but also reduces post-yield toughness (Currey, 2002), but no studies have found variations in bone mineral density between proximal and distal limb midshafts (Ruff and Hayes, 1984).

This study examines two additional and potential adaptations for limb tapering, modeling and Haversian remodeling for the following reasons. First, they are probably the most labile osteogenic responses to loading that generate phenotypically plastic variations in cortical bone shape and strength. Second, how cortical bone modulates modeling and Haversian remodeling has been a longstanding problem, especially for understanding how bones age and maintain structural variations.

Modeling

Modeling (defined here in a narrow sense as the addition of bone mass) increases resistance to bending by augmenting I around the axes in which applied forces generate deformation so that a given moment generates less strain (Wainright et al., 1976). Because I depends on the squared distance of each unit area from the neutral axis of bending, bones should optimize I relative to mass by adding bone periosteally and removing it endosteally (expanding the medullary cavity), yielding a high ratio of diameter (D) to wall thickness (t), Marrow, however, whose density is roughly 50% of bone, limits the optimum D/t ratio in mammals to approximately 4.6 to maximize stiffness relative to mass (Pauwels, 1974; Alexander, 1981; Currey and Alexander, 1985). Among terrestrial mammals, the median ratio of D/t is approximately 4.4, with a higher median value for the femur (5.4) and lower values for the humerus and more distal limb elements (Currey and Alexander, 1985). There is abundant evidence in juveniles that modeling increases I in response to loading, mostly through increases in periosteal apposition (Chamay and Tchantz, 1972; Goodship et al., 1979; Lanyon et al., 1982; Lanyon and Rubin, 1984; Rubin and Lanyon, 1984a,b, 1985; Biewener et al., 1986; Raab et al., 1991; Lieberman, 1996; Bass et al., 1998; Ruff et al., 1994; Lieberman and Pearson, 2001), and to a lesser extent through inhibition of endosteal resorption (Woo et al., 1981). To evaluate modeling effects on I as a means of compensating for distal tapering, however, more data are needed on strains in proximal *versus* distal midshafts during conditions of loading that are within biologically normal ranges and without the potentially confounding effects of surgical intervention (see Bertram and Swartz, 1991). Obviously distal bones do not usually model as much as proximal bones (otherwise they would have similar cortical thickness), but it is not known if differences in strain environments account for differences in modeling rates.

Haversian remodeling

Another potential adaptation to limb tapering may be to increase Haversian remodeling (HR) rates in distal *versus* proximal elements. During HR, osteoclasts first resorb old bone, and osteoblasts then lay down concentric lamellae of new bone around a central vascular channel. The function of HR is not entirely understood (see Martin et al., 1998; Currey, 2002), but it is generally thought that it prevents or repairs fatigue damage caused by high strain magnitudes and/or frequencies. Although Haversian (secondary osteonal) bone is weaker *in vitro* than young primary osteonal bone (Currey, 1959; Carter and Hayes, 1977a,b; Vincentelli and Grigorov, 1985), it is apparently stronger than old, microcrack-damaged primary bone (Schaffler et al., 1989, 1990). Haversian systems may also prevent or halt microfracture propagation. In addition, HR can strengthen bone by reorienting more collagen along axes of tension (Martin and Burr, 1982; Riggs et al., 1993a,b). A number of studies demonstrate that loading increases remodeling rates (Hĕrt et al., 1972; Bouvier and Hylander, 1981, 1996; Churches and Howlett, 1981; Rubin and Lanyon, 1984b, 1985; Schaffler and Burr, 1988; Burr et al., 1985; Mori and Burr, 1993; Lieberman and Pearson, 2001; Lees et al., 2002; for a review, see Goodship and Cunningham, 2001). In addition, HR preferentially occurs in older regions of long bones that have presumably accumulated the most damage (Frost, 1973; Bouvier and Hylander, 1981; Currey, 2002).

The possibility that HR is an adaptation for maintaining tapered distal limbs has been suggested but never been tested comprehensively. Lieberman and Crompton (1998) found higher rates of HR in distal than proximal midshafts in juvenile swine, and Lieberman and Pearson (2001) found higher rates of HR in distal than proximal midshafts in juvenile sheep.

However, these studies did not relate rates of HR to differences in strain environments, and only examined juveniles.

The optimization model

Here we test the general hypothesis that limbs trade-off modeling *versus* remodeling responses to loading in cortical bone to maximize strength relative to the cost of adding mass. We focus on modeling and HR rates in relation to strain data solely in the midshafts of the femur, tibia and metatarsal for three reasons. (1) Midshafts are the location of peak bending, so the locations are biomechanically comparable (see Biewener et al., 1986). (2) Variations in loading regime elsewhere in diaphyses, especially near epiphyses, are currently unknown. (3) In sheep the second hind-limb segment is simpler to model than the forelimb because it has only one bony element, the tibia.

The general prediction is that if bones optimize strength relative to the cost of adding mass, and if HR repairs or prevents microdamage, then the proportions of modeling *versus* HR responses to loading should vary at different skeletal locations and ages in relation to their costs and benefits (Fig. 1). As noted above, the major mechanical benefit of modeling is to strengthen a bone by increasing the second moment of area around the axes in which bending forces generate deformation. The major long-term cost of modeling, however, is the additional energy required to accelerate added mass during swing, a cost that should be approximately proportional to mR^2, where m is the mass of the limb, and R is the distance from the center of mass (COM) of the limb to the hip or shoulder joint (Hildebrand, 1985; Winter, 1990). Adding bone mass distally will not only increase the limb's mass but will also move the limb's COM distally (increasing R). Because cost is proportional to R^2, small increases in R may have large effects.

The costs and benefits of HR are less understood, but differ from those of modeling. As noted above, proposed benefits of HR include replacing and thereby strengthening fatigue-damaged bone, increasing elasticity, and halting microfracture propagation without adding mass or changing shape (Martin et al., 1998; Schaffler et al., 1990; Currey, 2002). But HR occurs slowly, increases porosity, and incurs higher long-term metabolic costs than modeling by leaving a bone insufficiently strong to resist further strain damage, requiring subsequent growth or remodeling (Martin, 1995).

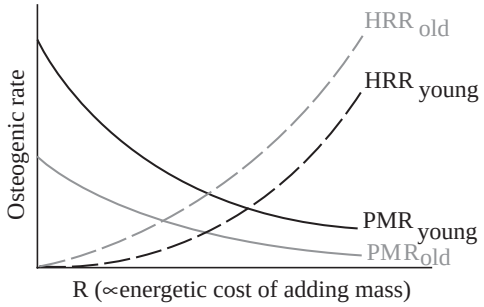

Fig. 1. Optimization model for cortical bone responses to loading. The periosteal modeling rate (PM RATE) is predicted to decrease and the Haversian remodeling rate (HRR) to increase with higher costs of adding mass [roughly proportional to R, the functional distance from each midshaft to the axis of rotation of the hind limb at the hip]. If Haversian remodeling functions to repair or prevent fatigue damage, then HRR is expected to increase as PM RATE activity declines with age for both models.

One additional issue to be considered is the effect of age. As osteoprogenitor cells senesce, they decline in number and become less sensitive to many epigenetic stimuli, including those from mechanical loading (Muschler et al., 2001; Chan and Duque, 2002). *In vitro* and comparative studies indicate that osteoblasts are less responsive to strains in older individuals (Erdmann et al., 1999; Stanford et al., 2000; Donahue et al., 2001). In addition, mechanical loading stimulates osteogenesis mostly prior to skeletal maturity, and primarily acts to slow down the rate of bone loss in older individuals (e.g. Ruff et al., 1994; Bass et al., 1998; Wolff et al., 1999; Kohrt, 2001).

Four specific hypotheses are tested. (1) While rates of periosteal growth are known to be less in distal than proximal midshafts (otherwise distal elements would not be thinner), rates of additional growth in response to loading are predicted to be less in distal than proximal elements. The null hypothesis is that rates of additional midshaft periosteal growth in response to loading are either similar between elements or vary in proportion to magnitudes of strain. (2) Because distal elements have thinner cortices than proximal elements (due to lower baseline rates of modeling), strain magnitudes should be higher in midshafts of distal elements compared to more proximal elements. The null hypothesis is that peak strain magnitudes should be similar between elements. (3) If HR is an adaptation to either prevent or repair fatigue damage caused by high strains, then rates of HR are predicted to be higher in distal than proximal elements because of increased strains in distal elements (hypothesis 2). The null hypothesis is that rates of HR at midshafts in response to loading are similar between elements. (4) If HR functions to repair or prevent fatigue damage, then rates of HR at midshafts should increase with age to compensate for decreased rates of modeling in response to mechanical loading. The null hypothesis is that HR rates at midshafts do not vary with age.

Materials and methods

Subjects and exercise treatment

Dorset sheep *Ovis aries* L. were used because they are docile, good treadmill runners, and have relatively little muscle mass on the tibia and metatarsal, permitting application of strain gauges at multiple sites without impairing normal gait (strain measurements from the femoral midshaft were not attempted). Two samples of sheep were used: one to compare the effects of exercise on bone growth and remodeling, the other to quantify bone strain. The first sample comprised juvenile (aged 40 days, N=10), subadult (aged 265 days,

N=10), and young adult (aged 415 days, *N*=16) sheep, divided into equal-sized sedentary control and exercise treatment groups for 90 days. Food, housing and other variables were held constant, except for exercise treatment (see Konieczynski et al., 1998). Exercised animals were run on a treadmill for 60 min·day^{-1} at a constant relative speed (Froude number), $\hat{u}$ of 0.5, defined $\hat{u}$ as $v^2(\boldsymbol{g}\,h)^{-0.5}$, where v is velocity, $\boldsymbol{g}$ is the gravitational constant and h is hip height. For most of the sheep, this speed was approximately 1.4–1.8 m s^{-1}, a moderate trot just above the walk–trot gait transition, resulting in approximately 6000 additional loading cycles per day. During the treatment period, fluorochrome dyes (Calcein, 20 mg kg^{-1}; Oxytetracyline, 50 mg kg^{-1}; Xylenol Orange, 25 mg kg^{-1}) were administered every 30 days *via* intraperitoneal injection to label added or remodeled bone. The first dye (Calcein) was administered after 1 week of training. Body mass was measured weekly. Animals were killed at the end of the experimental period. Interarticular lengths of the femur, tibia and metatarsal were measured *post mortem* using digital calipers. Femoral length was measured from the most proximal point on the femoral head to the intercondylar line; tibial length was measured from the center of the lateral condylar surface to the center of the distal articular surface; metatarsal length was measured from the center of the proximal articular surface to the most distal point of the distal articular surface.

An additional sample of five juvenile Dorset sheep approximately 40 days old were used for strain gauge analyses. These animals were the same age and body mass (20–30 kg) as the juvenile group described above prior to treatment period. The animals were trained to run on a treadmill at 1.5 m s^{-1}, a trotting gait corresponding to a Froude number of 0.5 and thus comparable to the above-described sample. Strains in these animals therefore approximate the pattern and magnitude of strain in the juvenile sample of exercised *versus* non-exercised Dorset sheep at the start of the exercise treatment period.

Histological analyses

For the exercised and control sheep, modeling and HR during the treatment period were quantified *post-mortem* on midshaft sections of the femur, tibia and metatarsal, stained and dehydrated in a solution of 1% basic Fuchsin in ethanol for 7 days, embedded in poly-methyl methacrylate, and cut into two sections. Each section was mounted to a glass slide, ground to a 100 μm-thick section, coverslips placed on top and analyzed using an Olympus SZH-10 microscope (Olympus America, Melville, NY, USA) with epifluorescence. Sections were digitized using a SPOT 1.3 digital camera (Diagnostic Instruments, Sterling Heights, MI, USA).

Haversian systems formed during the fluorochrome-labeled treatment period were counted in each quadrant using Image Pro-Plus (Media Cybernetics, Silver Spring, MD, USA). We could not label the first two phases of Haversian remodeling (activation and resorption), but the dyes enabled us to determine if the onset of the third phase, formation, occurred during the treatment period. Thus Haversian systems were not counted if the outer (first) layer of Haversian bone was not labeled with fluorochome dye. Haversian systems activated before the treatment period could not be excluded, but these were assumed to be the same for both treatment groups (i.e. before the exercise treatment period). HR density was calculated as the total number of initiated Haversian systems/cross-sectional area; HR rate was calculated as the total number of initiated Haversian systems/cross-sectional area/treatment day. Periosteal area (PA) added was measured using NIH Image v1.62 (http://rsb.info.nih.gov/nih-image/) as the total area added during the treatment period from the initial Calcein line, which marked the first day of the experiment, to the outer cortex of the bone. PA added was standardized by body mass; Periosteal modeling (PM) rate was calculated as PA added/treatment day.

Strain and kinematic recordings

Rosette strain gauges were surgically attached to three locations around the midshaft of the tibia in five juveniles and the metatarsal in three juveniles of the strain-gauge sheep sample (see above). Prior to surgery, subjects were sedated with ketamine (8.0 mg kg^{-1}, i.m.), xylazine (0.05 mg kg^{-1}, i.m.) and atropine (0.05 mg kg^{-1}, i.m.), intubated, and maintained on a surgical plane of anaesthesia with isofluorane. The left hind limb of each animal was shaved and sterilized, and the location of the midshaft marked. Under sterile surgical conditions, insulated FRA-1-11 rosette strain gauges (Sokki Kenkyujo, Tokyo, Japan) of 120±0.5 Ω resistance were affixed to the cranial, medial and caudal surfaces of the tibial midshaft through an incision on the medial surface, and to the cranial, medial and lateral surfaces of the metatarsal midshaft from incisions on the medial and lateral surfaces of the foot (in one sheep, no. 574, the cranial gauge was positioned on the craniomedial surface). Gauges were sealed using M-coat and D-coat (MicroMeasurements Inc., Raleigh, NC, USA). To provide anaesthesia and minimize inflammation, Bupivacaine (diluted 1:10 v/v) was injected subcutaneously around each incision site. Muscles and tendons were retracted on the posterior and anterior surface of both bones during gauge insertion, but care was taken to ensure that these structures were not cut or damaged. The surface of the bone at each gauge site was prepared by cutting a small window (ca. 5 mm^2) in the periosteum, cauterizing any vessels, and degreasing with 100% chloroform. Bupivacaine (diluted 1:10 v/v) was perfused under the periosteum prior to cutting, to provide anaesthesia. Gauges were bonded using methyl-2-cyano-acrylate glue, with continuous pressure applied for 2 min as the glue was drying. Care was taken to align one of the elements of the gauge with the long axis of the bone. The orientations of each gauge's A-element (previously marked on the gauge's sealing coat using metallic ink) relative to the long axis of the bone was recorded prior to closing the incision with suture. Gauge leads were then passed extracutaneously underneath flexible bandages to the hip, where they were attached to a bandage loosely wrapped around the animal's abdomen. To provide strain relief, the leads of each gauge were affixed tightly to a bandage wrapped around the leg near the incision site.

Strain data were recorded 4 and 24 h after surgery, when animals were running with an apparently normal gait and showed no signs of lameness, distress or discomfort (e.g. with symmetrical limb kinematics on the operated and non-operated hind limbs and no signs of leaning or favoring one limb over another). During each recording session, the gauges were connected with insulated wire to Vishay 2120A amplifiers (MicroMeasurements Inc., Raleigh, NC, USA) to form one arm of a Wheatstone bridge in quarter-bridge mode; bridge excitation was 1 V. Voltage outputs were recorded on a TEAC™ RD-145T DAT tape recorder (TEAC™ Corp, Tokyo, Japan). Gauges were periodically balanced to adjust for zero offsets during the experiment, and calibrated when the animal was stationary with the instrumented leg unsupported.

To correlate strains with limb kinematics, 3-D coordinates were obtained for all hind-limb joints using an infrared motion analysis system (Qualisys Inc., East Windsor, CT, USA). Three cameras tracked the position of reflective markers (12 mm diameter) placed on the shaved skin overlying the distal interphalangeal joint, distal metatarsal, lateral malleolus, lateral epicondyle of the femur, greater trochanter and anterior superior iliac spine. Kinematic sequences captured at 60 Hz were synchronized to the strain gauge output, using a trigger that started data capture by the Qualysis system at the same time that a 2 V pulse signal was sent to the tape recorder. Limb segments were identified by connecting adjacent markers. QTools software (Qualisys Inc., East Windsor, CT, USA) was used to identify temporal midstance and measure element orientation at midstance.

Strain gauge analyses

Selected sequences of strain data were sampled from the tape recorder on a Macintosh G4 computer using an Ionet™ A-D board (GW Instruments, Somerville, MA, USA) at 250 Hz. A Superscope 3.0™ (GW Instruments, Somerville, MA, USA) virtual instrument (written by D.E.L.) was used to determine the zero offset, and calculate strains (in microstrain, με) from raw voltage data using shunt calibration signals recorded during the experiment. For each gauge, principal tension (ε_1), compression (ε_2), and the orientation of principal tensile strain ($\varepsilon_1°$) relative to the bone's long axis, were calculated following equations in Biewener (1992). Igor Pro v. 4.0 (Wavemetrics Inc., Lake Oswego, OR, USA) was used to calculate these strains at temporal midstance (when peak strain occurs) for at least 10 gait cycles for each animal. In some cases, not all elements of the gauge were working, but we were able to use the calibrated strain values from the element aligned with the long axis of the bone to approximate normal strain (see below).

To characterize midshaft strain environment in the tibia and metatarsal, digitized transverse cross-sections of each midshaft were analyzed with a macro (written by S. Martin, University of Melbourne, Australia) for NIH Image to calculate and graph the neutral axis (NA) and gradients of normal strain across the section, under two assumptions: that the bone shafts are beams loaded axially and in bending, and that the strain distribution is linear (formulae in Rybicki et al., 1974; Biewener, 1992; Gross et al., 1992). These isoclines were used to estimate the magnitude of peak maximum (tensile) and minimum (compressive) normal strains at the cortex of the midshaft of the tibia and metatarsal. In several animals for which isoclines could not be calculated for the tibia (see Table 5), maximum strains were estimated from the cranial gauge, and minimum strains were approximated from the caudal gauge. Since the tibia is bent around a mediolateral axis at midstance (see below), these approximations were considered reasonable. Strain due to bending and axial compression was calculated following equations in Biewener (1992). Digitized cross-sections in conjunction with coordinates of the experimentally determined NA were also used to calculate the polar moment of inertia, J, the sum of any two orthogonal second moments of area (I) around a neutral axis through the area centroid, and Z_c, the section modulus of compression, using an additional macro for NIH Image 1.62 (written with the help of S. Martin). The macro works by calculating I_N as the sum of the areas of each pixel times its squared distance to the neutral axis. Z_c was calculated as I_N/a_c, where a_c is the greatest perpendicular distance from the neutral axis to the outer perimeter subject to compression in the plane of bending. This program was also used to calculate J and cross-sectional areas for the juvenile, subadult and adult sample of exercised *versus* control sheep. Cross-sectional properties were standardized by body mass and element length.

Results

Modeling and Haversian remodeling rates

Tables 1 and 2 summarize data on total periosteal area (PA) added (standardized by body mass) and the number of added Haversian systems (HR density, standardized by cross-sectional area) in the exercise and sedentary treatment groups

Table 1. *Effects of exercise and age on midshaft periosteal area added during treatment period*

		Periosteal area added ($mm^2\ kg^{-1}$)		
	N	Femur	Tibia	Metatarsal
Juvenile				
Controls	5	1.19±0.12	0.67±0.08^{F}	0.61±0.09^{T,F}
Runners	5	**1.61±0.29**	**1.11±0.21**^{F}	0.74±0.17^{F}
Subadult				
Controls	5	1.25±0.23	1.02±0.02	0.84±0.26^{F}
Runners	5	1.44±0.19	**1.17±0.10**^{F}	0.91±0.06^{T,F}
Adult				
Controls	8	0.24±0.09	0.12±0.05^{F}	0.07±0.03^{F}
Runners	8	0.27±0.14	0.16±0.10	0.16±0.14^{F}

Values are means ±1 S.D.

Mann–Whitney U test: ^{F}significantly different from femur ($P<0.05$); ^{T}significantly different from tibia ($P<0.05$).

Values in **bold** are significantly different from controls ($P<0.05$).

Table 2. *Effects of exercise and age on number of Haversian systems added at midshaft during treatment period*

		Added Haversian density (secondary osteons mm^{-2})		
	N	Femur	Tibia	Metatarsal
Juvenile				
Controls	5	0.04±0.05	2.34±1.13^{F}	7.89±2.26^{T,F}
Runners	5	0.05±0.05	**4.67±2.79**^{F}	**16.31±4.71**^{T,F}
Subadult				
Controls	5	0.04±0.04	0.95±0.76^{F}	6.33±4.05^{T,F}
Runners	5	0.05±0.06	**3.15±1.52**^{F}	11.08±7.45^{T,F}
Adult				
Controls	8	0.42±0.38	8.76±6.82^{F}	21.42±9.66^{T,F}
Runners	8	0.40±0.26	9.03±5.35^{F}	22.02±14.64^{T,F}

Values are means ± 1 S.D.

Mann–Whitney *U* test: ^{F}significantly different from femur (P<0.05); ^{T}significantly different from tibia (P<0.05).

Values in **bold** are significantly different from controls (P<0.05).

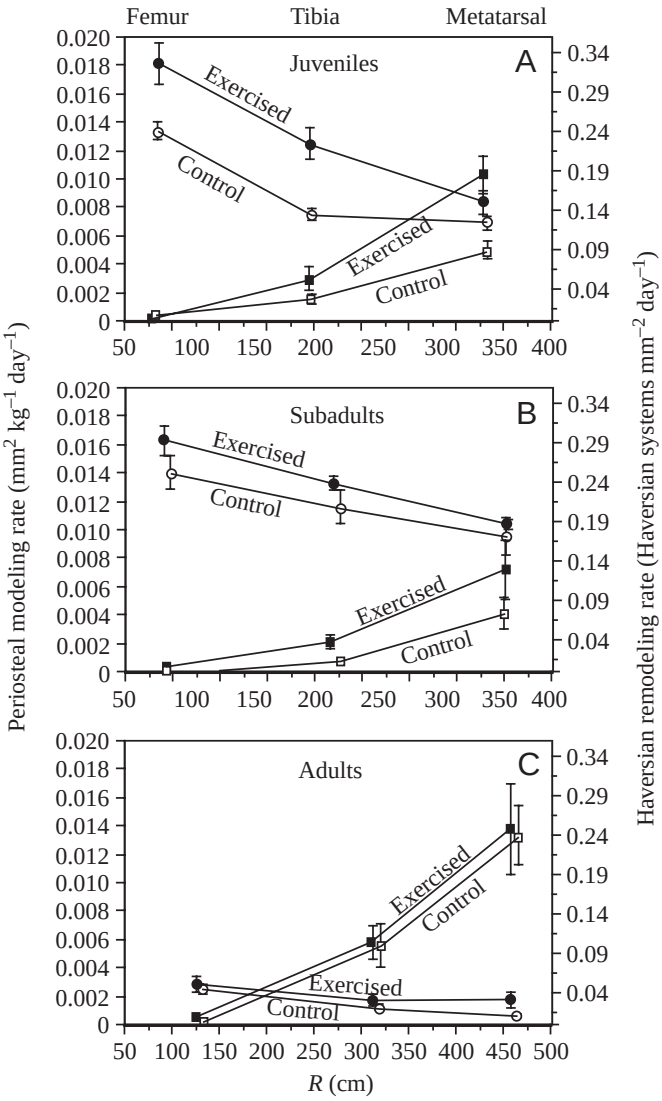

Fig. 2. Midshaft periosteal modeling rate (left *y*-axis, circles), and Haversian remodeling rate (right *y*-axis, squares) *versus* *R*, the distance from the midshaft to the hip joint (*x*-axis) in juveniles (A), subadults (B) and young adults (C). Runners, filled symbols; controls, unfilled symbols. Values are means ±1 S.E.M. The energetic cost of added mass is approximately proportional to the square of *R*. Modeling rates are higher in proximal than distal bones, and decrease with age, whereas remodeling rates are higher in distal than proximal bones, and increase with age. The effects of exercise are greatest in juveniles, and non-significant in all adults. See Tables 1 and 2 for tests of significance.

for all three ontogenetic stages. In Fig. 2 these results are shown as rates of the periosteal modeling (PM; added periosteal area kg^{-1} day^{-1}) and HR rate (added Haversian systems mm^{-2} day^{-1}), against *R*, the functional distance between each midshaft and the hip joint measured at midstance. As noted above, *R* does not measure the inertia of the limb during swing phase but should be roughly proportional to this parameter. These results indicate that exercise-induced loading affected both modeling and HR, but in different proportions in each element midshaft by age. PA added (Table 1) and PM rate (Fig. 2) at the midshaft decline from proximal to distal in juveniles and subadults, but not in young adults (in which PM rates in all midshafts are close to zero). Statistically significant (P<0.05) increases in PA added at the midshaft as a result of exercise are evident in the juvenile femora and tibiae but not in the metatarsals; a similar trend of decreasing exercise effect on PA added and PM rate from proximal to distal midshafts is evident in the subadult sample, but is not statistically significant in the femur or the metatarsal. Adults show no significant periosteal modeling response to exercise in any midshaft element.

Table 2 and Fig. 2 also indicate that HR densities and HR rates at the midshaft vary inversely with modeling rates. All age groups show a marked increase in HR density and HR rate in distal *versus* proximal midshafts, but with considerably higher HR rates in adults than juveniles (P<0.05). Exercise effects on HR are greatest in juveniles, and decline during ontogeny. No statistically significant effect of exercise on HR density was found in adults in any midshaft. In the femur and tibia of the control animals, Haversian systems were absent or rare in juveniles and subadults, and at low densities in adults. Haversian densities were higher in the metatarsals than the tibia or femur at all ages, particularly in the adult controls. Thus, at least in immature animals, exercise exaggerated an existing trend of higher HR rates in distal *versus* proximal midshafts. The spatial distribution of Haversian systems (by quadrant) differed between bones, but was not significantly different between runners and controls. In the juveniles, 100% of added Haversian systems in the femur were in the caudal quadrant; in the tibia, 98% were in the cranial and medial quadrants; and in the metatarsal, 52% were in the cranial quadrant, and 18% and 20% in the medial and lateral quadrants, respectively.

Table 3. *Comparison of standardized midshaft cross-sectional properties*

		Cortical area *CA* ($mm^2\ kg^{-1}$)			Polar moment of inertia, *J* ($mm^4\ kg^{-1}\ l^{-1}$)		
	N	Femur	Tibia	Metatarsal	Femur	Tibia	Metatarsal
Juvenile							
Controls	5	3.45±0.42	3.17±0.25	2.51±0.26^{T,F}	0.98±0.15	0.53±0.08^{F}	0.49±0.05^{T,F}
Runners	5	3.57±0.21	3.55±0.22	2.66±0.26^{T,F}	1.11±0.11	**0.67±0.09^{F}**	**0.60±0.11^{T,F}**
Subadult							
Controls	5	3.71±0.40	3.33±0.26	2.53±0.24^{T,F}	1.27±0.15	0.65±0.08^{F}	0.65±0.10^{T,F}
Runners	5	3.63±0.27	3.41±0.17	2.53±0.12^{T,F}	1.17±0.15	0.64±0.05^{F}	0.64±0.05^{F}
Adult							
Controls	8	3.23±0.41	3.76±0.30^{F}	1.96±0.17^{T,F}	1.28±0.20	0.59±0.08^{F}	0.50±0.07^{F}
Runners	8	3.48±0.33	2.91±0.22^{F}	**2.34±0.25^{T,F}**	1.30±0.31	0.59±0.08^{F}	0.57±0.10^{F}

Values are means ± 1 S.D.
Mann–Whitney *U* test: ^{F}significantly different from femur ($P<0.05$); ^{T}significantly different from tibia ($P<0.05$).
Values in **bold** are significantly different from controls ($P<0.05$).

Table 3 summarizes some effects of periosteal modeling rates on bone cross-sectional properties during ontogeny in the control *versus* exercised sheep sample (endosteal resorption rates could not be measured in this study). Cortical area *CA*, standardized by body mass, which indicates bone strength in compression, is greater in proximal than distal midshafts. Mass- and length-standardized measurements of the polar moment of inertia, *J*, an indicator of overall resistance to bending and torsion in fairly symmetrical cross-sections such as these (Wainright et al., 1976), is approximately 15% smaller in the metatarsal *versus* tibia, and approximately 50% smaller in the tibia *versus* femur.

Midshaft strains

Tables 4 and 5 summarize normal strains and the orientation of principal strains from gauge sites at midstance, along with calculated maximum and minimum normal strains on the cortex and total bending strain for 10 typical strides at 1.5 m s^{-1} from the metatarsal and tibia (no strain data were obtained for the femur). Not all elements were working in several gauges, as noted in Tables 4 and 5, in which case longitudinal strains (strains from the element aligned with the bone's long axis) were substituted for normal strains (no calculations of the orientation of tension are possible for these gauges). Note that in the metatarsal of one animal (no. 539), the medial gauge was located on the tensile side of the NA, whereas in the other two individuals (nos. 574 and 616), the medial gauge was located more cranially, on the compressive side of the NA. In addition, all the tibial gauges worked simultaneously in only one animal (no. 600). However, of the five animals with tibial strain data, at least three gauges worked from each site, and the results are similar between individuals (see Table 5). In particular, all gauges on the caudal and medial cortices experienced compressive normal strains, with much higher values on the caudal cortex; all gauges on the cranial cortex experienced tensile normal strains; and measurements of maximum principal strain angle at each site do not vary greatly. The relative magnitudes of normal strain between all gauge sites are approximately similar, indicating a strain regime of bending in the sagittal plane combined with axial compression (which shifts the neutral axis towards the cortex subject to tension). Fig. 3 illustrates typical cross-sectional strain isoclines for both midshafts using mean normal strains calculated for each gauge site and representative cross sections (nos. 600 for the tibia, 539 for the metatarsal).

As shown in Fig. 3, at midstance, both the metatarsal and the tibia are primarily bent around a neutral axis that is oriented within 10° of a mediolateral axis, but is shifted towards the caudal aspect of the metatarsal and the cranial aspect of the tibia. Both the tibia and metatarsal have higher compressive than tensile strains, as one would expect for a loading regime that combines bending with axial compression (Wainright et al., 1976). The maximum and minimum normal strains in the metatarsals are 50–70% higher than maximum and minimum strains in the tibia. The metatarsal not only experiences substantially higher strains, but also appears to experience relatively more compression (more tibial data are needed to confirm this). Relative to the (assumed vertical) ground reaction force in the sagittal plane at midstance, mean orientation of the tibia is 29±4.5° (proximal end angled cranially), and mean orientation of the metatarsal is 14±2.7° (proximal end angled caudally). Principal strain orientations (ε_1°) correspond with a loading regime characterized primarily by bending. Principal tension on the cortices in compression (cranial in the metatarsal, caudal in the tibia) is within 15° of the expected 90° (Tables 3 and 4). Principal tension on the cranial (tensile) cortex of the tibia is within a maximum of 26° of the expected 0° (Table 5). In addition, the orientation of tension on the medial cortex of the tibia is within 10° of the expected 45° angle at which it should cross the neutral axis under bending (Table 5); however, the angles of ε_1° on the medial and lateral cortices of the metatarsal are more variable (Table 4), possibly reflecting variations in gauge positions relative to the neutral axis in this bone.

Table 4. *Metatarsal midstance strain data at 1.5 m s^{-1} for 10 strides*

	Cortex						Normal strain ε_1				
	Cranial		Medial		Lateral						
Animal	ε_1	ε_1°	ε_1	ε_1°	ε_1	ε_1°	Maximum[1]	Minimum[2]	Axial strain[3]	Bending strain[4]	% bending
574	–672.9 (±37.6)†	–84.4 (±1.2)	–23.5 (±40.5)	55 (±1.9)	42.8 (±29.0)	–30.9 (±0.6)	700	–1300	–300	±1000	77
539	–1291.5 (±36.1)*	–	77.9 (±32.5)	–35.8 (±3.3)	149.8 (±19.4)	–19.2 (±2.5)	700	–1350	–325	±1025	76
616	–1124.6 (±91.4)	–89.2 (±0.2)	–79.4 (±34.7)	73.1 (±6.1)	171.6 (±38.2)	–23.9 (±1.0)	625	–1225	–300	±925	75
Mean	–1029.6 (±320.1)	–87.6 (±4.5)	–8.41 (±79.7)[1]	30.81 (±58.4)‡	121.4 (±69.0)	–24.7 (±5.9)	675 (±43)	–1292 (±63)	–308.3 (±14.4)	±983.3 (±52.0)	76

Values in parentheses for individual subjects are standard deviations for 10 separate stance phases.
Grand mean standard deviation is calculated from individual subject means.
*Longitudinal strain (from single element aligned with long axis).
†Gauge was located on craniomedial rather than cranial cortex.
‡High standard deviations are the result of different gauge position relative to the neutral axis in animal 539 than in 574 and 616.
[1]Maximum normal strain isocline on plantar cortex.
[2]Minimum normal strain isocline on cranial cortex.
[3]Calculated as (maximum+minimum normal strain)/2.
[4]Calculated as absolute value of (minimum –maximum normal strain)/2.
ε_1, normal strain.
ε_1°, orientation of tensile strain (degrees).

Table 6 summarizes the section moduli of compression (Z_C) calculated around the experimentally determined neutral axis, the polar moment of inertia (J), and cortical area (CA) along with data on body mass and element length for the juveniles for which cross-sectional strains normal to the midshaft (Tables 4 and 5) could be calculated (note that these sheep are 90 days younger and roughly half the body mass of the post-treatment juveniles summarized in Table 1). Although complete data are available for only one tibia (no. 600), the consistency of strain results among gauges from Table 5

Fig. 3. Isoclines of strains (ε) in microstrain (με) in the midshaft cross section of the tibia (A) and metatarsal (B) of two juvenile sheep at 1.5 m s^{-1}. NA is the neutral axis; positive ε values are tensile, negative ε values are compressive. × indicates the location of rosette strain gauges and arrows show the orientation of the principal strain (ε_1°) relative to the bone's long axis. Orientations of strains (solid lines) relative to the long axis of the bone (dotted lines) are indicated by the small figures adjacent to each gauge site. Both bones are bent in the sagittal plane, with neutral axes shifted significantly from the cross-sectional centroid towards the cortex subject to tension.

suggests that this is a reasonable, representative tibia (a hypothesis that needs further testing). The cross-sectional properties accord with the differences in strain documented above for the tibia and metatarsal in several respects. First, *CA* standardized by body mass is roughly 1.5 times greater in the tibia, causing greater resistance to axial compression; axial compression is also expected to be less in the tibia because it is loaded less vertically at midstance (see above). In addition, although section moduli of compression (Z_c, standardized by element length and body mass) are comparable between the tibia and metatarsal, the tibia has a 20% greater overall strength than the metatarsal as indicated by *J* (standardized by element length and body mass). These differences are similar in pattern (although slightly different in value) to comparisons of length and mass standardized *J* for the exercised *versus* control samples summarized above in Table 3.

Discussion

The above results are consistent with the general hypothesis that the responses of cortical bone to loading vary in such a way as to optimize strength relative to cost in juveniles, but not in adults. Four specific hypotheses were tested. First, rates of growth in response to loading were hypothesized to be less in distal than proximal element midshafts, in proportion to *R*. This hypothesis is supported, but only in juveniles in which periosteal modeling (PM) rates in the controls are significantly less in distal midshafts than proximal midshafts. In addition, the effect of exercise on PM rate was higher in proximal midshafts (the femur and tibia) than distal midshafts (the metatarsal). With increasing age, rates of periosteal growth decrease in the controls, as do any exercise effects on PM rate. These results are in general agreement with several previous studies of the effects of mechanical loading on cortical bone growth (summarized above), but without the potentially confounding effects of trauma or otherwise abnormal responses to non-habitual levels of types of loading (Bertram and Swartz, 1991). One exception is Woo et al. (1981), who found that exercise inhibited endosteal resorption but had no effect on periosteal growth rates in the femora of growing miniature swine exercised for 6 km day^{-1} for about 1 year. Lieberman (1996) and Lieberman and Crompton (1998), however, found that exercise did significantly increase cortical bone growth in limb midshafts of minature swine exercised twice daily for 30 min each for 90 days compared to controls. Further study is necessary to understand these differences.

The juvenile results also support the hypothesis that HR rate in response to loading is higher in distal than proximal element midshafts. HR rate in the controls is higher in proximal than distal midshafts at all ages, with essentially no activation of HR in femoral midshafts, and several

Table 5. *Tibia midstance strain data at 1.5 m s^{-1} for 10 strides*

	Cortex						Normal strain ε_1				
	Cranial		Medial		Lateral						
Animal	ε_1	ε_1°	ε_1	ε_1°	ε_1	ε_1°	Maximum	Minimum	Axial strain[5]	Bending strain[6]	% Bending
616	–428.5 (±51.3)*	–	–	–	553.2 (±60.0)	26.8 (±0.9)	553[1]	–429[3]	–62	±491	89
574	–	–	–215.2 (±46.4)	53.2 (±1.6)	556.6 (±100.8)	–14.8 (±2.1)	557[1]	–			–
562	–	–	–449.4 (±71.8)	49.9 (±1.3)	–	–	–	–			–
539	–748.3 (±77.9)*	–	–312.4 (±52.4)	54.4 (±0.8)	–	–	–	–748[3]			–
600	–759.6 (±42.7)	–76.4 (±0.9)	–191.7 (±42.1)	50.7 (±1.4)	441.4 (±35.0)	–12 (±2.0)	445[2]	–760[4]	–157.5	±602.5	79
Mean	–645.5 (±188)	–76.4 (NA)	–292.2 (±117.1)	52.1 (±2.1)	517.1 (±65.6)	–17.9 (±7.9)	518 (±64)	–646 (±188)	–64	±582	90

Values in parentheses for individual subjects are standard deviations for 10 separate stance phases.
Grand mean standard deviation is calculated from individual subject means; NA, not applicable.
*Longitudinal strain (from single element aligned with long axis).
[1]Maximum normal strain estimated from cranial gauge.
[2]Maximum normal strain isocline on cranial cortex.
[3]Minimum normal strain estimated from caudal gauge.
[4]Maximum normal strain isocline on caudal cortex.
[5]Calculated as (maximum+minimum normal strain)/2.
[6]Calculated as absolute value of (minimum –maximum normal strain)/2.
ε_1, normal (principal) tensile strain.
ε_1°, orientation of tensile strain (degrees).

Table 6. *Cross-sectional properties of tibia and metatarsals in strain-gauged sheep*

Individual	Bone	Body mass (kg)	J (kg^{-1} l^{-1})	Z_C (kg^{-1} l^{-1})	CA (kg^{-1})
539	Metatarsal	18.5	0.69	0.60	3.39
574	Metatarsal	18.6	0.73	0.71	3.89
616	Metatarsal	18.2	0.72	0.75	3.68
600	Tibia	18.9	0.85	0.61	5.38

J, polar moment of inertia calculated around area centroid (standardized by body mass and element length).

Z_C, section modulus relative to cortex under compression (standardized by body mass and element length), calculated as I_N/a_c, where I_N is the second moment of area around the neutral axis NA and a_c is the perpendicular distance from NA to the location of peak compression on the periosteal cortex.

CA, cortical area (standardized by body mass).

times higher HR rates in the tibia and metatarsal midshafts. In the juveniles, HR rate in response to exercise increases significantly in the tibia and metatarsal, but not in the femur. The effect of exercise is less in the subadult sample and non-existent in the adult sample. Viewed together, the data for HR and PM rates from the juvenile sample indicate the existence of a trade-off in which modeling rates decrease from proximal to distal midshafts, while HR rates increase from proximal to distal midshafts. Mechanical loading exaggerates this trade-off, stimulating proportionate increases of periosteal growth in the proximal midshafts and of HR in the distal midshafts.

A related hypothesis is that strain magnitudes should be higher in distal than proximal midshafts, since they have smaller cross-sections, and because HR may repair bone but does not augment cross-sectional strength. This is supported by the data from the strain-gauged juveniles. No femoral strains were measured, but the sum of bending and compressive strain in the metatarsal is approximately twice that in the tibia at midstance. While the metatarsal is loaded more axially than the tibia (at midstance it is inclined approximately 15° closer to vertical), the higher metatarsal strains are most likely to be attributable to smaller cross-sectional areas and second moments of areas (further research is necessary to test for effects of muscle loads exerted on these midshafts, such as the metatarsal–phalangeal joint extensors). The trade-off between periosteal modeling and HR, in combination with higher metatarsal strains, therefore suggests that distal midshafts are adapted to be lighter at the expense of strength. This hypothesis, however, needs to be further tested with femoral strain data, which we predict to be even lower than in the tibia because of the femur's much greater cross-sectional strength (Table 3). Strain data from animals at later ontogenetic stages are also needed.

The results also support the fourth hypothesis, that HR rate increases with age to compensate for decreased rates of modeling in response to loading. In the sheep studied here, periosteal modeling rates decline with age, whereas HR rates increase with age. However, while exercise effects on modeling decline with age, it is interesting that exercise effects on HR also decline with age. There are several potential explanations for this finding. One possibility is that HR fails to be stimulated at an increased rate by loading in older animals, but acts as a preventative mechanism to halt microcrack propagation. Alternatively, the loads in this experiment may have been too low to stimulate HR, a possibility suggested by the results of Lees et al. (2002), in which ulnar osteotomies in adult sheep induced higher microcrack rates and higher HR rates in the proximal radius. Lees et al. (2002), however, did not measure *in vivo* strains.

Finally, the results also test the mechanostat hypothesis (Frost, 1987, 1990), which predicts that HR is inhibited when modeling is stimulated (and *vice versa*), and that rates of HR should be lower in midshafts subject to higher strain magnitudes, and higher in midshafts subject to lower strains. The above results do indicate a trade-off between modeling and HR in response to loading, but in the opposite direction predicted by the mechanostat (higher modeling rates in the metatarsal, subjected to higher strains, and higher rates of HR in the tibia, subjected to lower strains).

We conclude that in comparisons of midshafts, cortical bone in the juvenile limb optimizes strength relative to the cost of adding mass by trading-off growth *versus* remodeling. Distal midshafts grow less than more proximal midshafts, saving energy costs associated with accelerating the limbs during the swing phase (Hildebrand, 1985; Myers and Steudel, 1985). The amount of energy saved by distal tapering is difficult to estimate accurately, but should be proportional to the reduction in skeletal mass in distal *versus* proximal elements. The periosteal growth rate in response to loading is lower for the metatarsal than the tibia, causing the metatarsal to have a thinner cortex and lower section moduli to resist bending. To estimate how much metatarsal mass was saved through reduced growth, we calculated the increase in area and compressive section modulus that is necessary to reduce the compressive strains due to axial compression and bending in the metatarsal to the same magnitudes as in the tibia (approx. 40% lower). This effect of tapering was calculated using basic engineering proportionalities for compression and bending: $\varepsilon_c \propto F/A$ and $M_b/\varepsilon_c \propto I_N/a_c$ (Hibbeler, 1999), where ε_c is compressive strain, F is the axial force, A is the cross-sectional area, M_b is the bending moment, I_N is the second moment of area relative to the neutral axis, and a_c is the perpendicular

distance from the neutral axis to the location of peak compression on the periosteal cortex. For a given axial force, a reduction in compressive strain by 40% requires an increase in cross-sectional area by 40%; for a given bending moment, a reduction in compressive strain due to this bending moment requires an increase of I_N/a_c (which is equal to Z_c) by 40%. Assuming the metatarsal is a hollow cylinder and its area and section modulus increase by periosteal apposition (with no endosteal expansion), the requisite increase in area and section modulus as well as the associated increase in volume/mass can be calculated from standard geometric formulae:

$$A = \pi\left[\left(\frac{D}{2}\right)^2 - \left(\frac{d}{2}\right)^2\right],$$

$$\frac{I_N}{a_c} = \frac{(\partial/64)\,(D^4 - d^4)}{a_c}$$

and

$$V = \pi\left(\frac{D}{2}\right)^2 l - \pi\left(\frac{d}{2}\right)^2 l,$$

where A = area, D = outer diameter, d = inner diameter of hollow cylinder, I_N = second moment of area, a_c = perpendicular distance from neutral axis to outer perimeter of cortex in compression, V = volume ($\propto$mass) and l = length of cylinder.

In order to augment the area of the juvenile sheep metatarsal sufficiently to decrease compressive strains from axial compression to the same magnitude as in the tibia, the diameter of the metatarsal would have to increase by 12%, which leads to an increase in volume/mass by 38%. In order to reduce compressive strains due to bending to tibia strain levels, the diameter of the metatarsal would have to increase by 10%, increasing the volume/mass of the metatarsal shaft by 33%. An alternative way to estimate the mass saved by distal tapering is to compare growth rates in response to loading. If one models the metatarsal as a cylinder, then its mass would have increased by approximately 12% if it grew at the same rate as the tibia in response to loading during the experiment (90 days). Over the same time period, its mass would have increased 30% if it grew at the same rate as the femur in response to loading.

The results of this study are therefore consistent with the hypothesis that limb bones initially trade-off the rate of growth *versus* HR responses to loading, thereby adapting bones to dissimilar strain environments. In particular, lighter, thinner distal limb bones apparently adapt to higher strains, and may do so in part with higher rates of HR. However, the results of this study have several limitations with regard to the hypothesis of optimization. Most importantly, while the trade-off between growth and HR accords with the predictions of optimization of strength relative to the cost of swinging mass, the differences evident between hind-limb midshafts may simply reflect variable osteogenic responses to different stimuli. We think this explanation can only be partially true. While higher rates of HR in the metatarsal *versus* tibial or femoral midshafts are probably a function of higher strains, HR alone is unlikely to increase midshaft strength in response to strains. The finding that higher strains in the metatarsal elicit lower rather than higher rates of modeling than in the tibia supports previous findings that distal bones are adapted to a higher point on the stress–strain curve and have lower safety factors (Vaughan and Mason, 1975; Alexander, 1981). Thus, if modeling alone maintains equilibrium at particular sites (Rubin and Lanyon, 1984a; Biewener et al., 1986; Carter and Beaupré, 2001), then it is possible that equilibrium thresholds vary between elements in order to optimize strength relative to the cost of adding mass. This hypothesis, however, needs to be tested further with data on strain magnitudes at multiple skeletal elements throughout ontogeny.

A second issue is that the optimization hypothesis tested here should not only apply to variations between bones but also within bones. Many (but not all) limb diaphyses are tapered (excluding the portions closest to distal epiphyses), and future analyses need to test for a trade-off between modeling and HR between proximal and distal portions of the shaft in such bones. A difficulty with testing this hypothesis is the challenge of characterizing the diaphyseal strains away from midshafts, especially toward the proximal ends, which tend to be heavily muscled, and are thus presumably subject to high local muscle forces (as well as difficult to instrument with strain gauges).

A third problem is that while higher HR rates in distal midshafts appear to correlate with higher magnitudes of strain, the above results do not test the presumed adaptive function of HR to repair, halt or possibly prevent load-induced microdamage. We are studying these possibilities further by quantifying rates of midshaft microdamage. A recent study of adult sheep (Lees et al., 2002) found increases in both microfracture and HR densities in the proximal radius following ulnar osteotomies, with peak HR density after 10 weeks. These data do not address whether microdamage is necessary to stimulate HR.

A final issue is that the effects of age on the apparent trade-off between periosteal modeling and HR observed here cannot be explained by optimization. Most notably, the results presented above indicate that while periosteal modeling rates decline with age in all limb midshafts, HR rates increase, but eventually level off. These observations accord with previously published data on bone growth rates and HR density in various adult mammals, including humans (e.g. Kerley, 1965; Ruff et al., 1994; Martin et al., 1998), and with evidence for reduced sensitivity to mechanical stimuli with age (Rubin et al., 1992; Turner et al., 1995). However, the effects of exercise in this study correlate with slight but non-significant differences in periosteal modeling and HR rates in the subadult sheep sample, and stimulated neither process in the young adult sheep. This interaction between age and exercise is difficult to explain with the data we collected. One possibility, which needs to be tested by quantifying microcrack density, is that levels of loading examined in this study were too low to stimulate HR. If so, increased rates of HR observed in adult sheep relative to juvenile sheep may be a preventative mechanism to halt

microcrack propagation rather than an adaptive response to repair microcracks. This hypothesis could be tested by analyzing HR rates along with microcrack damage in adult sheep subjected to more vigorous loading. An additional possibility is that the lack of any significant HR or periosteal modeling response to exercise in adult sheep is a mechanobiological constraint caused by skeletal senescence. Older bone tissue may not be able to respond to strains, perhaps because osteoblasts are less responsive to strain stimuli (Rubin et al., 1992; Turner et al., 1995; Muschler et al., 2001; Chan and Duque, 2002), and because older bone cells (probably osteocytes) may be less able to transduce strain signals. Analyses of midshafts in humans and beagles indicate that the density of microcracks increases with age, while the HR activation frequency declines, along with osteocyte density (Vashishth et al., 2000; Frank et al., 2002).

These results also have implications for efforts to reconstruct habitual behaviors from variations in cross-sectional bone geometry in humans and other vertebrates, based on the principle that second moments of area quantify cross-sectional resistance to loading (see Lieberman et al., in press). Cross-sectional shape responses to loading vary by skeletal location, and primarily reflect stimuli prior to skeletal maturity. In addition, since distal midshafts respond less to mechanical loading than proximal midshafts, proximal elements such as the femur or humerus may be more sensitive indicators of mechanical loading than more distal elements such as the metapodia.

Finally, variable cortical bone responses to loading have several important evolutionary and clinical implications. From an evolutionary perspective, the trade-off between growth and remodeling provides support for the hypothesis that natural selection tends to drive physiological systems towards more efficient use of energy (Weibel et al., 1991; Alexander, 1996). Ontogenetic changes in the trade-off between cortical bone growth *versus* remodeling are also clinically significant for evaluating the role of load-bearing exercise in osteoporosis. The ontogenetic shift documented here supports studies (e.g. Turner et al., 1995; Stanford et al., 2000), showing that mechanical usage prior to skeletal maturity results in permanently stronger bones; after skeletal maturity, moderate load-bearing exercise appears to have little measurable effect on activating periosteal modeling or HR, but may make the remodeling process more efficient by generating osteons with smaller Haversian channels and less porous bone (Thompson, 1980). Future work, therefore, is needed to address what stimuli elicit HR, and how intermediary mechanisms modulate variable osteogenic responses to loading.

List of symbols and abbreviations

A	cross sectional area
a_c	greatest perpendicular distance from NA to outer perimeter
CA	cortical area
COM	center of mass
D	outer diameter
d	inner diameter
F	axial force
$\boldsymbol{g}$	gravitational constant
GRF	ground reaction force
h	hip height
HR	Haversian remodeling
I	second moments of area
J	moment of inertia
l	limb (element) length
M	body mass
M_b	bending moment
m	mass of limb
NA	neutral axis
PA	periosteal area
PM	periosteal modeling
R	distance from COM of limb to hip or shoulder joint
t	wall thickness
$\hat{u}$	constant relative speed (Froude number)
v	velocity
V	volume
Z_c	modulus of compression
ε_1	principal tension
$\varepsilon_1°$	orientation of principal tensile strain
ε_2	compression
$\mu\varepsilon$	microstrain

This work was supported by NSF IBN 96-03833 to D.E.L., and the American Federation for Aging Research. We thank F. Bidlack, R. Bernstein, M. Devlin, K. Rafferty, P. Ramirez, M. Toscano, L. Tuanquin for their assistance. We are grateful to A. Biewener, D. Burr, B. Richmond and two anonymous reviewers for comments, and to the late C. Richard Taylor who initially inspired the research.

References

Alexander, R. McN. (1977). Terrestrial locomotion. In *Mechanics and Energetics of Animal Locomotion* (ed. R. McN. Alexander and G. Goldspink), pp. 168-203. London: Chapman and Hall.

Alexander, R. McN. (1980). Optimum walking techniques for quadrupeds and bipeds. *J. Zool., Lond.* **173**, 549-573.

Alexander, R. McN. (1981). Factors of safety in the structure of animals. *Sci. Prog., Oxford* **67**, 109-130.

Alexander, R. McN. (1996). *Optima for Animals*. Princeton University Press.

Bass, S., Pearce, G., Bradney, M., Hendrich, E., Delmas, P. D., Harding, A. and Seeman, E. (1998). Exercise before puberty may confer residual benefits in bone density in adulthood: studies in active prepubertal and retired female gymnasts. *J. Bone Min. Res.* **13**, 500-507.

Bertram, J. E. A. and Biewener, A. A. (1988). Bone curvature: sacrificing strength for load predictability? *J. Theor. Biol.* **131**, 75-92.

Bertram, J. E. A. and Biewener, A. A. (1992). Allometry and curvature in the long bones of quadrupedal mammals. *J. Zool., Lond.* **226**, 455-467.

Bertram, J. E. A. and Swartz, S. M. (1991). The 'law of bone transformation': a case of crying Wolff? *Biol. Rev. Camb. Phil. Soc.* **66**, 245-273.

Biewener, A. A. (1983). Allometry of quadrupedal locomotion: the scaling of duty factor, bone curvature and limb orientation to body size. *J. Exp. Biol.* **105**, 147-171.

Biewener, A. A. (1991). Musculoskeletal design in relation to body size *J. Biomech.* **24**, 19-29.

Biewener, A. A. (1992). In vivo measurement of bone strain and tendon force. In *Biomechanics – Structures and Systems: A Practical Approach* (ed. A. A. Biewener), pp. 123-147. Oxford: Oxford University Press.

Biewener, A. A., Swartz, S. M. and Bertram, J. E. A. (1986). Bone modeling during growth: Dynamic strain equilibrium in the chick tibiotarsus. *Calc. Tiss. Int.* **39**, 390-395.

Biewener, A. A., Thomason, J., Goodship, A. and Lanyon, L. E. (1983). Bone stress in the horse forelimb during locomotion at different gaits: a comparison of two experimental methods. *J. Biomech.* **16**, 565-576.

Biewener, A. A., Thomson, J. and Lanyon, L. E. (1988). Mechanics of locomotion and jumping in the horse (*Equus*); *in vivo* stress in the tibia and metatarsus. *J. Zool., Lond.* **214**, 547-565.

Bouvier, M. and Hylander, W. L. (1981). Effect of bone strain on cortical bone structure in macaques (*Macaca mulatta*). *J. Morphol.* **167**, 1-12.

Bouvier, M. and Hylander, W. L. (1996). The function of secondary osteonal bone: Mechanical or metabolic? *Arch. Oral Biol.* **41**, 941-950.

Burr, D. B., Martin, R. B., Schaffler, M. B. and Radin, E. L. (1985). Bone remodeling in response to *in vivo* fatigue microdamage. *J. Biomech.* **18**, 189-200.

Carter, D. R. and Hayes, W. C. (1977a). Compact bone fatigue damage – a microscopic examination. *Clin. Orthop. Rel. Res.* **127**, 265-274.

Carter, D. R. and Hayes, W. C. (1977b). Compact bone fatigue damage – I. Residual strength and stiffness. *J. Biomech.* **10**, 323-337.

Carter, D. R. and Beaupré, G. S. (2001). *Skeletal Form and Function: Mechanobiology of Skeletal Development, Aging and Regeneration*. Cambridge: Cambridge University Press.

Chamay, A. and Tchantz, P. (1972). Mechanical influences in bone remodeling. Experimental research on Wolff's Law. *J. Biomech.* **5**, 173-180.

Chan, G. K. and Duque, G. (2002). Age-related bone loss: old bone, new facts. *Gerontology* **48**, 62-71.

Churches, A. E. and Howlett, C. R. (1981). The response of mature cortical bone to controlled time-varying loading. In *The Mechanical Properties of Bone* (ed. S. C. Cowin), pp. 69-80. New York: ASME.

Currey, J. D. (1959). Differences in the tensile strengths of bone of different histological types. *J. Anat.* **93**, 87-95.

Currey, J. D. (2002). *Bones: Structure and Mechanics*. Princeton: Princeton University Press.

Currey, J. D. and Alexander, R. M. (1985). The thickness of the walls of tubular bones. *J. Zool., Lond.* **206A**, 453-468.

Donahue, S. W., Jacobs, C. R. and Donahue, H. J. (2001). Flow-induced calcium oscillations in rat osteoblasts are age, loading frequency, and shear stress dependent. *Am. J. Physiol. Cell Physiol.* **281**, C1635-C1641.

Erdmann, J., Kogler, C., Diel, I., Ziegler, R. and Pfeilschifter, J. (1999). Age-associated changes in the stimulatory effect of transforming growth factor beta on human osteogenic colony formation. *Mech. Ageing Dev.* **110**, 73-85.

Frank, J. D., Ryan, M., Kalscheur, V. L., Ruaux-Mason, C. P., Hozak, R. R. and Muir, P. (2002). Aging and accumulation of microdamage in canine bone. *Bone* **30**, 201-206.

Frost, H. M. (1973). *Bone Remodeling and its Relation to Metabolic Bone Disease*. Springfield, IL: Charles C. Thomas.

Frost, H. M. (1987). Bone 'mass' and the 'mechanostat': A proposal. *Anat. Rec.* **219**, 1-9.

Frost, H. M. (1990). Skeletal structural adaptations to mechanical usage (SATMU). *Anat. Rec.* **226**, 403-422.

Gambaryan, P. P. (1974). *How Mammals Run: Anatomical Adaptations* (translated by H. Hardin). New York: Wiley.

Goodship, A. E. and Cunningham, J. L. (2001). Pathophysiology of functional adaptation of bone in remodeling and repair *in vivo*. In *Bone Mechanics Handbook*, 2nd edition (ed. S.C. Cowin), pp. 26-1–26-31. Boca Raton: CRC Press.

Goodship, A. E., Lanyon, L. E. and McFie, H. (1979). Functional adaptation of bone to increased stress. *J. Bone Jnt. Surg.* **61**, 539-546.

Gross, T. S., McLeod, K. J. and Rubin, C. T. (1992). Characterizing bone strain distributions *in vivo* using three triple rosette strain gauges. *J. Biomech.* **25**, 1081-1087.

Hěrt, J., Přybylová, E. and Lišková, M. (1972). Reaction of bone to mechanical stimuli, Part 3. Microstructure of compact bone of rabbit tibia after intermittent loading. *Acta Anat.* **82**, 218-230.

Hibbeler, R. C. (1999). *Mechanics of Materials*, 4th Edition. Upper Saddle River, NJ: Prentice Hall.

Hildebrand, M. (1985). Walking and Running. In *Functional Vertebrate Morphology* (ed. M. Hildebrand, D. M. Bramble, K. F. Liem and D. B. Wake), pp. 38-57. Cambridge: Harvard University Press.

Jungers, W. L. (1985). Body size and scaling of limb proportions in primates. In *Size and Scaling in Primate Biology* (ed. W. L. Jungers), pp. 345-381. New York: Plenum.

Kerley, E. R. (1965). The microscopic determination of age in human bone. *Am. J. Phys. Anthropol.* **23**, 149-164.

Kohrt, W. M. (2001). Aging and the osteogenic response to mechanical loading. *Int. J. Sport Nutr. Exerc. Metab.* **11 Suppl**, S137-S142.

Konieczynski, D. D., Truty, M. J. and Biewener, A. A. (1998). Evaluation of a bone's *in-vivo* 24-hour loading history for physical exercise compared with background loading. *J. Orthop. Res.* **16**, 29-37.

Lanyon, L. E. and Rubin, C. T. (1984). Static versus dynamic loading as an influence on bone remodeling. *J. Biomech.* **17**, 897-906.

Lanyon, L. E., Goodship, A. E., Pye, C. J and MacPhie, H. (1982). Mechanically adaptive bone remodeling. *J. Biomech.* **15**, 141-154.

Lees, T. C., Staines, A. and Taylor, D. (2002). Bone adaptation to load: microdamage as a stimulus for bone remodeling. *J. Anat.* **201**, 437-446.

Lieberman, D. E. (1996). How and why humans grow thin skulls: Experimental evidence for systemic cortical robusticity. *Am. J. Phys. Anthropol.* **101**, 217-236.

Lieberman, D. E. and Crompton, A. W. (1998). Responses of bone to stress. In *Principles of Biological Design: The Optimization and Symmorphosis Debate* (ed. E. Weibel, C. R. Taylor and L. Bolis), pp. 78-86. Cambridge: Cambridge University Press.

Lieberman, D. E. and Pearson, O. M. (2001). Trade-off between modeling and remodeling responses to loading in the mammalian limb. *Bull. Mus. Comp. Zool.* **156**, 269-282.

Lieberman, D. E., Polk, J. D. and Demes, B. (in press). Predicting long bone loading from cross-sectional geometry. *Am. J. Phys. Anthropol.*

MacKelvie, K. J., Khan, K. M. and McKay, H. A. (2002). Is there a critical period for bone response to weight-bearing exercise in children and adolescents? A systematic review. *Br. J. Sports Med.* **36**, 250-257.

Martin, R. B. (1995). Mathematical model for repair of fatigue damage and stress fracture in osteonal bone. *J. Orthop. Res.* **13**, 309-316.

Martin, R. B. and Burr, D. B. (1982). A hypothetical mechanism for the stimulation of osteonal remodeling by fatigue damage. *J. Biomech.* **15**, 137-139.

Martin, R. B., Burr, D. B. and Sharkey, N. (1998). *Skeletal Tissue Mechanics*. New York: Springer.

Mori, S. and Burr, D. B. (1993). Increased intracortical remodeling following fatigue damage. *Bone* **16**, 103-109.

Muschler, G. F., Nitto, H., Boehm, C. A. and Easley, K. A. (2001). Age- and gender-related changes in the cellularity of human bone marrow and the prevalence of osteoblastic progenitors. *J. Orthop. Res.* **19**, 117-125.

Myers, M. J. and Steudel, K. (1985). Effect of limb mass and its distribution on the energetic cost of running. *J. Exp. Biol.* **116**, 363-373.

Pauwels, F. (1974). Über die Bedeutung der Markhöhle für die mechanische Beanspruchung des Röhrenknochens. *Z. Anat. Entwickl.-Gesch.* **145**, 81-85.

Polk, J. D. (2002). Adaptive and phylogenetic influences on musculoskeletal design in cercopithecine primates. *J. Exp. Biol.* **205**, 3399-3412.

Raab, D. M., Crenshaw, T. D., Kimmel, D. B. and Smith, E. L. (1991). A histomorphometric study of cortical bone activity during increased weight-bearing exercise. *J. Bone Min. Res.* **6**, 741-749.

Riggs, C. M., Lanyon, L. E. and Boyde, A. (1993a). Functional associations between collagen fibre orientation and locomotor strain direction in cortical bone of the equine radius. *Anat. Embryol.* **187**, 231-238.

Riggs, C. M., Vaughan, L. C., Evans, G. P., Lanyon, L. E. and Boyde, A. (1993b). Mechanical implications of collagen fibre orientation in cortical bone of the equine radius. *Anat. Embryol.* **187**, 239-248.

Rubin, C. T. and Lanyon, L. E. (1984a). Dynamic strain similarity in vertebrates: an alternative to allometric limb bone scaling. *J. Theor. Biol.* **107**, 321-327.

Rubin, C. T. and Lanyon, L. E. (1984b). Regulation of bone formation by applied dynamic loads. *J. Bone Joint Surg.* **66**, 397-402.

Rubin, C. T. and Lanyon, L. E. (1985). Regulation of bone mass by mechanical strain magnitude. *Calc. Tiss. Int.* **37**, 411-417.

Rubin, C. T., Bain, S. D. and McLeod, K. J. (1992). Supression of osteogenic response in the aging skeleton. *Calc. Tissue Int.* **50**, 306-313.

Ruff, C. B. and Hayes, W. C. (1984). Age changes in geometry and mineral content of the lower limb bones. *Ann. Biomed. Eng.* **12**, 573-584.

Ruff, C. B., Walker, A. and Trinkaus, E. (1994). Postcranial robusticity in *Homo*. III: Ontogeny. *Am. J. Phys. Anthropol.* **93**, 35-54.

Rybicki, E. F., Simonen, F. A., Mills, E. J., Hassler, C. R., Scoles, P., Milne, D. and Weis, E. B. (1974). Mathematical and experimental studies on the mechanics of plated transverse fractures. *J. Biomech.* **7**, 377-384.

Schaffler, M. B. and Burr, D. B. (1988). Stiffness of compact bone: effects of porosity and density *J. Biomech.* **21**, 13-16.

Schaffler, M. B., Radin, E. L. and Burr, D. B. (1989). Mechanical and

morphological effects of strain rate on fatigue of compact bone. *Bone* **10**, 207-214.

Schaffler, M. B., Radin, E. L. and Burr, D. B. (1990). Long-term fatigue behavior of compact bone at low strain magnitude and rate. *Bone* **11**, 321-326.

Smith, J. M and Savage, R. J. G. (1956). Some locomotory adaptations in mammals. *Zool. J. Linn. Soc.* **42**, 603-622.

Stanford, C. M., Welsch, F., Kastner, N., Thomas, G., Zaharias, R., Holtman, K. and Brand, R. A. (2000). Primary human bone cultures from older patients do not respond at continuum levels of *in vivo* strain magnitudes. *J. Biomech.* **33**, 63-71.

Taylor, C. R., Shkolnik, A., Dmi'el, R., Baharav, D. and Borut, A. (1974). Running in cheetahs, gazelle and goats: energy costs and limb configuration. *Am. J. Physiol*. **227**, 848-850.

Thompson, D. D. (1980). Age changes in bone mineralization, cortical thickness and Haversian canal area. *Calc. Tissue Int.* **31**, 5-11.

Turner, C. H., Takano, Y. and Owan, I. (1995). Aging changes mechanical loading thresholds for bone formation in rats. *J. Bone Min. Res*. **10**, 1544-1549.

Vashishth, D., Verborgt, O., Divine, G., Schaffler, M. B. and Fyhrie, D. P. (2000). Decline in osteocyte lacunar density in human cortical bone is associated with accumulation of microcracks with age. *Bone* **26**, 375-380.

Vaughan, L. C. and Mason, B. J. E. (1975). *A Clinico-Pathological Study of Racing Accidents in Horses*. Dorking: Batholomew Press.

Vincentelli, R. and Grigorov, M. (1985). The effect of Haversian remodeling on the tensile properties of human cortical bone. *J. Biomech.* **18**, 201-207.

Wainright, S. A., Biggs, B. A., Currey, J. D. and Gosline, J. M. (1976). *Mechanical Design in Organisms*. Princeton: Princeton University Press.

Weibel, E. R., Taylor, C. R. and Hoppeler, H. (1991). The concept of symmorphosis: a testable hypothesis of structure–function relationship. *Proc. Natl. Acad. Sci. USA* **88**, 10357-10361.

Winter, D. A. (1990). *Biomechanics and Motor Control of Human Movement*, 2nd edition. New York: Wiley.

Wolff, I., van Croonenborg, J. J., Kemper, H. C., Kostense, P. J. and Twisk, J. W. (1999). The effect of exercise training programs on bone mass: a meta-analysis of published controlled trials in pre- and postmenopausal women. *Osteoporosis Int.* **9**, 1-12.

Woo, S. L., Kuei, S. C., Amiel, D., Gomez, M. A., Hayes, W. C., White F. C. and Akeson, W. H. (1981). The effect of prolonged physical training on the properties of long bone: a study of Wolff's Law. *J. Bone Joint Surg. Am.* **63**, 780-787.